2. Seismic hazard and target spectra definition

The Yerba Buena Island is selected as the site of interest. It is in the San Francisco Bay Area, between two active crustal faults (e.g. the San Andreas and the Hayward faults), with global coordinates 37.82121° N and 122.37163° W. A site-specific probabilistic seismic hazard analysis (PSHA) was performed using the software package HAZ45 [21] (see Fig 1a). For this study the maximum considered earthquake (MCE) intensity level, corresponding to the UHS with a probability of exceedance of 2% in 50 years (TR = 2475 years) is selected as the seismic demand for seismic assessment. The MCE spectrum is transformed to a risk-adjusted spectrum using Method 2 of ASCE7-16§Ch16 [3]. The resulting spectrum is also known as Risk-targed Maximum Considered Earthquake (MCE_R), and is assumed to ensure an uniform probability of structural collapse of 1% in 50 years. Fig 1b compares the computed site-specific MCE and MCE_R along with the code-based MCE_R spectra defined as 3/2 of the design intensity level.

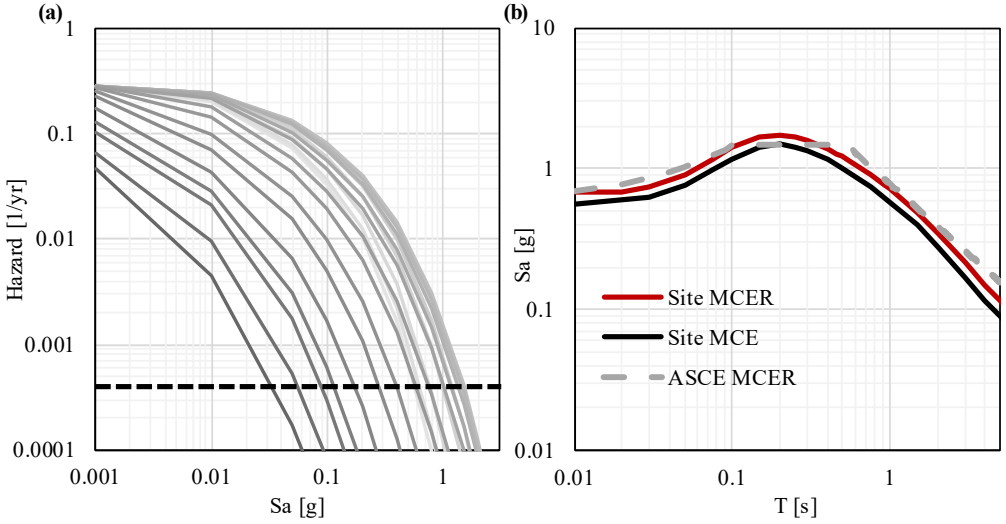

Fig 1- (a) Site specific hazard curves (b) MCE, Risk-adjusted MCE and code spectrum.

Fig 2 shows the deaggregation for magnitude (M_w) and distance (R_{rup}) for the 0.5, 1.5 and 2.0 s periods. The average values of magnitude and distance are M=7.10 and R= 16 km. These values are used to compute the mean and standard deviation of the ground motion models (GMM) needed to estimate the CMS.

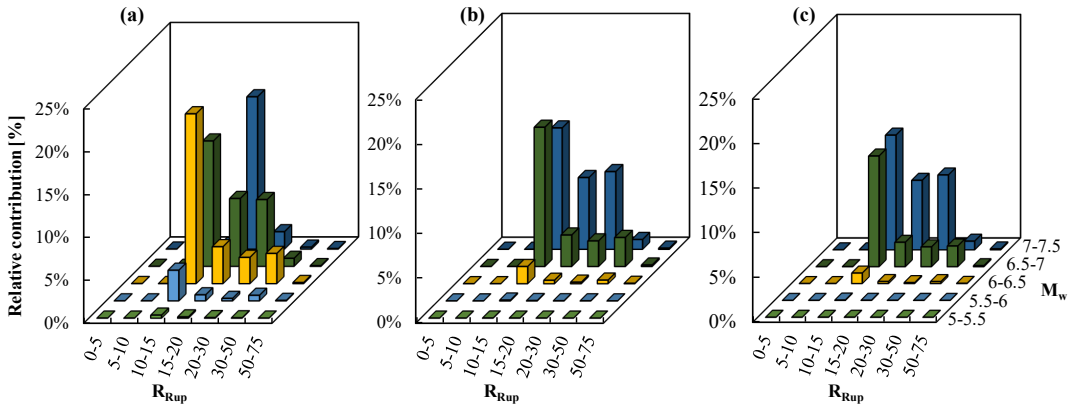

Fig 2 Deaggregation for the 2475-year return period earthquake for (a) T= 0.5 s (b) T= 1-50 s (c) T=2.0 s

Suites of CMS' are computed targeting the site-specific MCE_R presented in Fig 1b at 15 different conditional periods logarithmically distributed: T^* = [0.03, 0.05, 0.075, 0.10, 0.20, 0.30, 0.40, 0.53, 0.75, 1.0,

The design elastic model accounted for degraded stiffness of the structural elements due to seismic loading using the expected effective inertia due to cracking as recommended by ACI-318. Normal weight concrete, with nominal strength f'_c = 6 ksi was assumed for the design of beams and columns. Selected reinforcing steel is ASTM A706 with nominal yielding strength of f_y = 60 ksi. Seismic load effects on the structural members were estimated by means of the Equivalent Lateral Force (ELT) method as permitted by ASCE-7-16 for the type and height of the structure. The results of a modal analysis show that the first three structural periods of the model in the East-West direction are 1.75, 0.53 and 0.27 s, respectively. To prevent unrealistically large structural over strength factors, the structural elements sections were selected so that the maximum drift of the model was as close as possible to the maximum allowable story drift ratio (SDR) of 2% as defined by the ASCE 7-16 [3]. The final cross sections of the perimeter frames are: 32"x32" for columns and 22"x32" for seismic beams.

After defining the cross section of all structural members on the linear model, a two-dimensional inelastic mathematical model, representative of half the structure in the EW-direction, was constructed. The software package OpenSees version 3.03[30] was used as the modeling tool. The model was constructed using force-based nonlinear beam-column elements with concentrated plasticity and the ends. The nonlinear behavior of the materials and the axial-moment interaction on the columns are accounted for by using fiber sections assigned to the plastic hinges of each element. Corotational transformation is used to consider the geometric nonlinearity due to the expected large displacements. Elastic linear sections with cracked properties were assigned to the elements beyond the plastic hinge region. Fibers are assigned confined concrete, unconfined concrete, or steel material properties depending on their location within the elements cross section. The stress-strain relationship of the materials used on the fiber sections are presented in Fig 6.

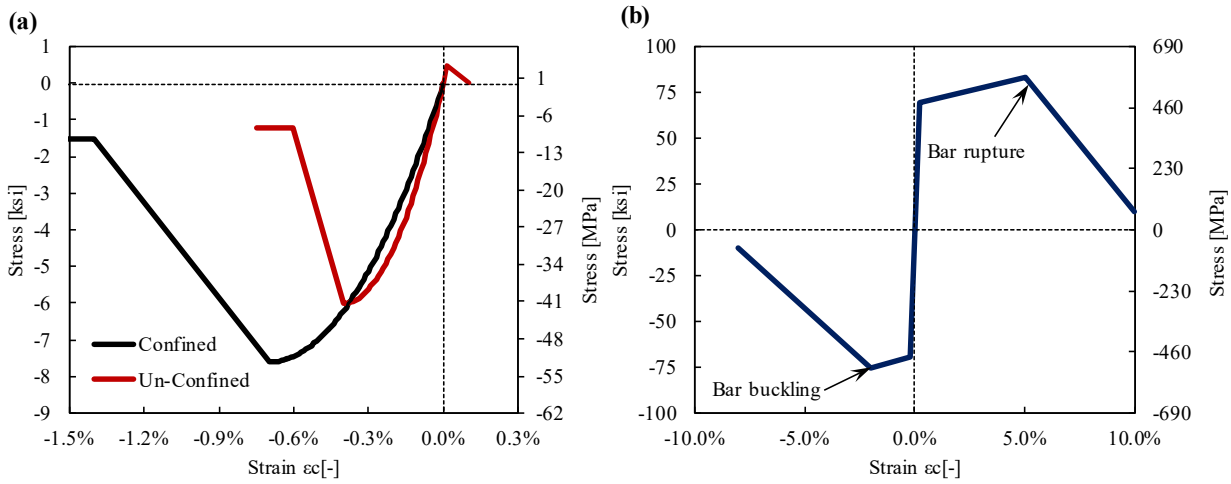

Fig 6 Materials stress-strain relation (a) Concrete (b) Reinforcement steel

Nonlinear static analyses (Pushover) are programed for estimating the model capacity. An inverse triangular load pattern approximates the distribution of the inertial forces under first-mode type of motion, and a rectangular load pattern is also implemented to simulate other plausible variations of the inertial-force distribution along the building height. The capacity curves of the building are presented in Fig 7a for each load pattern, the horizontal dashed line represents the design base shear normalized by the seismic weight (V_{bd}/W), which confirms an overstrength factor of approximately 1.5. To have a sense of the expected demand on the structure, Fig 7b shows the equivalent SDOF capacity curve[31] contrasted against the spectral displacement versus spectral acceleration spectrum (e.g. S_d vs. S_a) of the demand URS in Fig 1b. It is shown that the MCE_R spectrum does not cross the pushovers, hence it is expected that the structure undergoes nonlinear behavior under this intensity level.

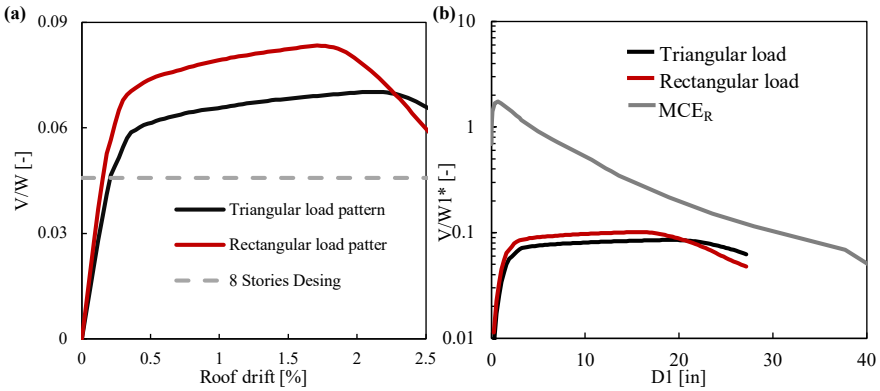

Fig 7 (a) Pushover and design base shear (b) Inelastic capacity Vs elastic demand

After applying the gravitational loads, an Eigen analysis was performed on the inelastic model to compute its periods. The obtained values for the first three vibration modes are 1.75, 0.53 and 0.3 s respectively. It is worth noting that these periods closely match the fundamental periods of the linear models with cracked sections. Moreover, the CMS' with $T^*=1.75$ and 0.53 were intentionally selected to match the fundamental periods of the nonlinear models.

5. Nonlinear response history analyses

With the selected ground motions, a total of 352 NL-RHA were performed. An example of the structural response distribution along height is presented in Fig 8. This figure represents the response of the model to the ground motions selected around the MCE_R. The thin red lines correspond to the response under each scaled ground motion. A total of 22 responses are plotted as the two-component of the 11 GM are used for the 2D analyses. The black continuous line represents the median of the 22 responses, the dashed line is the 84th percentile and the blue line is the elastic response obtained from the linear model. It is worth noting how the elastic shear demand is underestimated by the elastic model. This has been reported previously for frame-wall structures subject to seismic demand consistent with the design level earthquake by Arteta and Moehle [32]

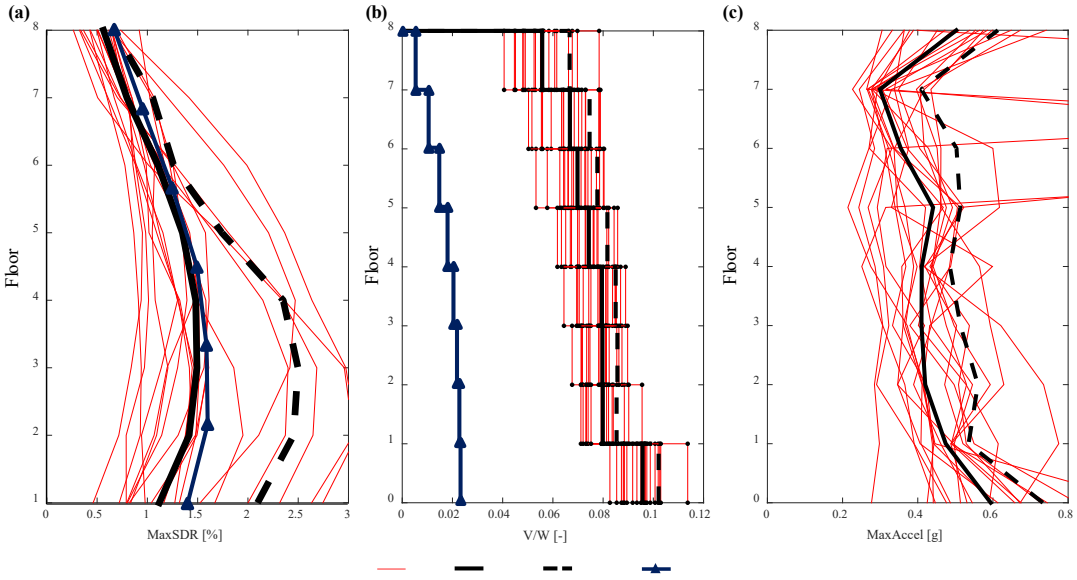

Fig 8 Distribution of EDP along height. (a) Displacement (b) Shear (c) Acceleration

Next, the structural response is evaluated for three different global summary EDPs: the maximum roof drift ratio (RDR_{max}), the maximum base shear normalized by the seismic weight (V_{bmax}/W), and the maximum total roof acceleration (TRA_{max}). To have a sense of the demand imposed on the models by the ground motions, the static pushover curves and the results of the nonlinear response history analysis are compared in Fig 9a using a scatter plot to represent the RDR_{max} and Vb_{max}/W results. As expected for the selected demand level, the accelerations induced on the structural model generate displacements that push the building into the nonlinear range. It is worth noting that the NL-RHA results are above the capacity curves because the distribution of inertial forces during a seismic event are different to the inverted triangular and rectangular load pattern used to compute the pushover curves. An alternative way of quantifying the nonlinearity demand in each model is presented in Fig 9b. This figure shows boxplots of the final period T_f of the structural model, normalized by the initial period of the nonlinear model for different target spectra. T_f is calculated by estimating the eigenvalues of the structure at the end of each analysis after the model ceases its displacements. As the mass remains constant, a lengthened final period will indicate a degradation of the stiffness caused by the incursion of the structure into the nonlinear range. It is noted that for $T^* > 0.4$ s, the median T_f remains invariant to the conditioning period, and is similar to that imposed by the runs under URS set. The average T_f obtained was 1.4 times the initial period of the structure.

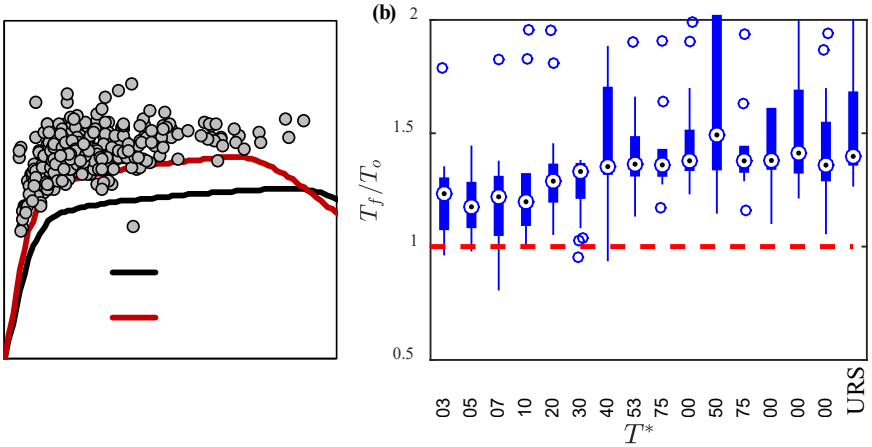

Fig 9 Static and dynamic analyses results (a) 4 stories model (b) 8 stories model (c) 16 stories model

To summarize the EDP result per ground motion set, boxplots are constructed with each set of 22 NL-RHA. For each EDP, 16 boxplots represent the response of the structure induced by the ground motions selected for each target spectra, including 15 variations of T^* for the CMS-based selections and 1 for the response under the set targeting the MCE_R. The x axis in the figures is the conditional period of the CMS normalized by either the cracked fundamental period of vibration (for displacement-related EDPs) (Fig 10a), or the second-mode period (for higher-mode dominated responses) (Fig 10b and Fig 10c). The period values used to normalize the conditional periods are those of the nonlinear models. A vertical dashed line show $T^*/T_i = 1$, to help compare the position of the maximum demand with respect to unity. A horizontal dashed line marks the median demand induced by the URS set.

Fig 10a shows that the median and variance of the displacement-related response of the structure is highly sensitive to the selection of T^*. As the conditioning period closely matches the fundamental period of the structure, larger are the displacements obtained. This confirms that the RDR_{max} EDP is a first-mode dominated response. It is worth noting that the median response under the MCE_R (tag as URS in Fig 10) ground motion set is comparable to the maximum median response obtained with the 15 CMS'. This result is against the hypothesis that the use of and enveloping spectra, such as the UHS or URS, for ground motion selection generates conservative results on the structural response. It is noted that, for the building and intensity level investigated, a GM selection for $T^* = T_f$ would have underestimated the maximum demand (see boxplots in the range $1.14 \leq T^*/T_i \leq 1.71$).

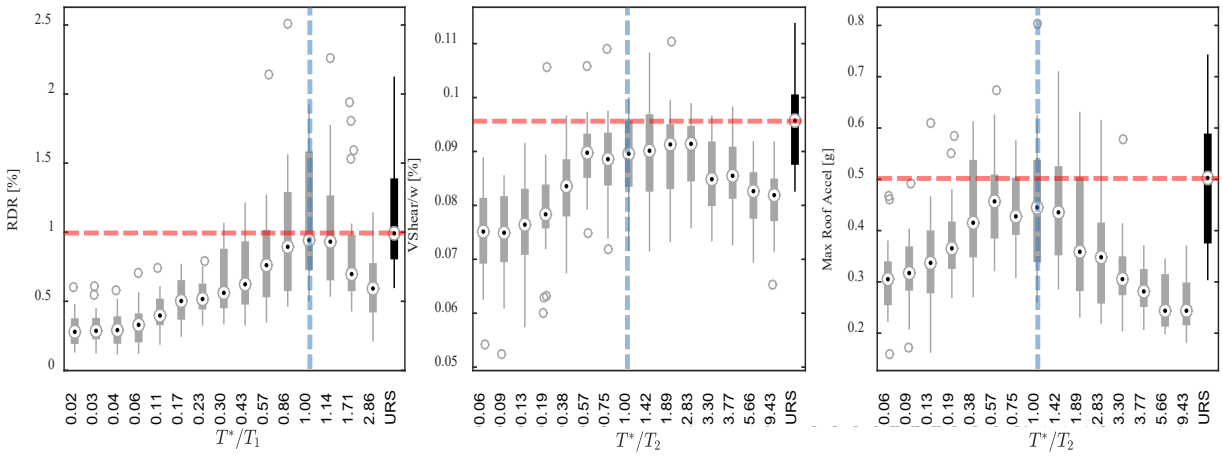

Fig 10 Variation of EDP with T^*(a) RDR_{max} (b) V_{bmax}/W (c) TRA_{max}

The distribution of maximum base shear presented in Fig 10b tends to be invariant over a range of conditional periods. This EDP is dominated by higher vibration modes as the maximum response is obtained near the second and third vibration mode of the structure. The maximum shear response is recorded in the range $0.5 \leq T^*/T_2 \leq 2.5$. It is noted that the use of a CMS conditioned at the first-mode period of the structure is not capable of capturing the maximum shear response and may lead to underestimations of this EDP. For example, see the results for T^*/T_2=3.30, which corresponds to the results conditioned at T_1. Comparing the median results obtained with the MCE_R and the median value of the CMS that produced the maximum shear response, is noted that the set of ground motions selected to match the MCE_R generate shear forces 5% higher than those of the maximum CMS set.

The TRA_{max} shows a distribution with a peak response at $T^*=0.3s$ ($T^*/T_2=0.57$) but is stable in the range $0.57 \leq T^*/T_2 \leq 1.47$ to then decreases for larger conditional periods. The median response of maximum roof accelerations generated by the ground motions selected around the MCE_R are 24% higher than those generated with the maximum CMS set. The period corresponding to the second vibration mode of the structure also shows to be a good estimation for T^* if the goal is to capture the maximum acceleration response, nevertheless, there might be some underprediction on the response.

6. Conclusions and recommendations

The conditional period value used for the ground motion selection, has a significant impact on the seismic response of the structure; the displacement-based EDP's are the most sensitive to the variation of T^*. If the analysis goal is to compute the maximum possible displacements, ground motions conditioned near the fundamental cracked period of the structure should be selected to perform the NL-RHA. For the case studied herein, the use of conditional periods far removed from the fundamental cracked one are not able to excite the structure and produce the displacements that a damaging seismic event could generate. Floor acceleration and base shear EDP's are underestimated when conditioning the CMS on fundamental cracked period of the structure. Conditioning periods around the second or third mode of vibration are more representative to estimate the maximum response of these EDP's

It is concluded that the use of only one CMS to assess the seismic response of a structure is not enough to produce the maximum values of all EDP's. When just one conditional period is used, only the frequencies near that period are excited; other vibration modes that contribute to the structural response are not excited. At least two CMS conditioned at different values are needed to capture the displacement, shear and acceleration responses accurately. Unlike the displacements, the base shear and floor acceleration maximum responses tends to remain constant over a wider range of conditioning periods, located around the second and

third vibration periods. Selecting ground motions for CMS's conditioned at T* within this range will produce, in practical terms, the same response for these EDP's.

The hypothesis that conservative structural responses are obtained when selecting ground motions based on enveloping spectra such as the UHS and URS, showed to be valid only for demand parameters that are triggered by frequencies higher than the first modal one. In the case of displacements, where the response is influenced by the fundamental mode, the mean response generated by the URS is very similar to the maximum response produced by the CMS conditioned at the optimal conditional period. A practical alternative for seismic evaluation could be to select and scale ground motions around the URS as specified by the design codes to perform the nonlinear response history analyses. Then, factor the results obtained by the relationship between the median value of the URS and the CMS that produce the maximum response. The results of this investigation suggest that these scaling factors for the EDP's in the nonlinear range are 1.0 for the displacements, 0.95 for the base shear and 0.80 for the maximum floor accelerations.

7. References

[1] National Research Council, "Selecting and Scaling Earthquake Ground Motions for Performing Analyses," 2015.

[2] Applied Technology Council, *Seismic Performance Assessment of Buildings, Volume 1, Methodology, FEMA P-58-1*, vol. 1, no. December. 2018.

[3] ASCE, *Minimum Design Loads and Associated Criteria for Buildings and Other Structures*. 2016.

[4] S. Kramer, *Geotechnical Earthquake Engineering*, First edit. Pearson, 1996.

[5] R. K. McGuire, *Seismic Hazard and Risk Analysis*. Earthquake Engineering Research Institute: Berkeley, 2004.

[6] N. Luco, B. R. Ellingwood, R. O. Hamburger, J. D. Hooper, J. K. Kimball, and C. a. Kircher, "Risk-targeted versus current seismic design maps for the conterminous united states," *Struct. Eng. Assoc. Calif. 2007 Conv. Proc.*, pp. 1–13, 2007.

[7] J. W. Baker, "Conditional Mean Spectrum: Tool for Ground-Motion Selection," *J. Struct. Eng.*, vol. 137, no. 3, pp. 322–331, 2011, doi: 10.1061/(asce)st.1943-541x.0000215.

[8] J. W. Baker and C. A. Cornell, "Spectral shape, epsilon and record selection," *Earthq. Eng. Struct. Dyn.*, vol. 35, no. 9, pp. 1077–1095, 2006, doi: 10.1002/eqe.571.

[9] J. . Bommer, S. . Scott, and S. . Sarma, "Hazard-consistent earthquake scenarios," *Soil Dyn. Earthq. Eng.*, vol. 19, no. 4, pp. 219–231, Jun. 2000, doi: 10.1016/S0267-7261(00)00012-9.

[10] B. Carlton and N. Abrahamson, "Issues and Approaches for Implementing Conditional Mean Spectra in Practice," *Bull. Seismol. Soc. Am.*, vol. 104, no. 1, pp. 503–512, 2014, doi: 10.1785/0120130129.

[11] F. Naeim and M. Lew, "On the Use of Desing Spectrum Compatible Time Histories.pdf," *Earthq. Spectra*, vol. Vol 11, pp. 111–127, 1995.

[12] Reiter.L, "Earthquake hazard analysis: Issues and insights," University Press, New York, 1990.

[13] C. A. Arteta and N. A. Abrahamson, "Conditional Scenario Spectra (CSS) for Hazard-Consistent Analysis of Engineering Systems," *Earthq. Spectra*, vol. 35, no. 2, pp. 737–757, 2019, doi: 10.1193/102116EQS176M.

[14] M. Kohrangi, D. Vamvatsikos, and P. Bazzurro, "Multi-Level Conditional Spectrum-Based Record Selection for Ida," in *Eleventh U.S. National Conference on Earthquake Engineering*, 2018.

[15] M. Kohrangi, P. Bazzurro, D. Vamvatsikos, and A. Spillatura, "Conditional spectrum-based ground motion record selection using average spectral acceleration," *Earthq. Eng. Struct. Dyn.*, vol. 46, no.

10, pp. 1667–1685, 2017, doi: 10.1002/eqe.

[16] K. Kolozvari, V. Terzic, R. Miller, and D. Saldana, "Assessment of dynamic behavior and seismic performance of a high-rise rc coupled wall building," *Eng. Struct.*, vol. 176, no. April, pp. 606–620, 2018, doi: 10.1016/j.engstruct.2018.08.100.

[17] N. Kwong and A. Chopra, "A Generalized Conditional Mean Spectrum and its application for intensity-based assessments of seismic demands," *Earthq. Spectra*, vol. 33, no. 1, pp. 123–143, 2017, doi: 10.1193/040416EQS050M.

[18] T. Lin, C. B. Haselton, and J. W. Baker, "Conditional spectrum-based ground motion selection . Part I : Hazard consistency for risk-based assessments," *Earthq. Eng. Struct. Dyn.*, vol. 42, no. 12, pp. 1847–1865, 2013, doi: 10.1002/eqe.

[19] P. Parra, C. Arteta, and J. Moehle, "Modeling criteria of older non - ductile concrete frame – wall buildings," *Bull. Earthq. Eng.*, no. 0123456789, 2019, doi: 10.1007/s10518-019-00697-y.

[20] B. A. Bradley, "A comparison of intensity-based demand distributions and the seismic demand hazard for seismic performance assessment," *Earthq. Eng. Struct. Dyn.*, vol. 42, no. 15, pp. 2235–2253, 2013, doi: 10.1002/eqe.2322.

[21] N. Abrahamson, "HAZ 45." github.com, 2016.

[22] J. W. Baker and N. Jayaram, "Correlation of spectral acceleration values from NGA ground motion models," *Earthq. Spectra*, vol. 24, no. 1, pp. 299–317, 2008, doi: 10.1193/1.2857544.

[23] N. A. Abrahamson, W. J. Silva, and R. Kamai, "Summary of the ASK14 Ground Motion Relation for Active Crustal Regions," *Earthq. Spectra*, vol. 30, no. 3, pp. 1025–1055, 2014, doi: 10.1193/070913EQS198M.

[24] K. W. Campbell and Y. Bozorgina, "NGA-West2 Ground Motion Model for the Average Horizontal Components of PGA , PGV , and 5 % Damped Linear Acceleration Response Spectra," *Earthq. Spectra*, vol. 30, no. 3, pp. 1087–1115, 2014, doi: 10.1193/062913EQS175M.

[25] D. M. Boore, J. P. Stewart, and G. M. Atkinson, "NGA-West2 Equations for Predicting PGA , PGV , and 5 % Damped PSA for Shallow Crustal Earthquakes," *Earthq. Spectra*, vol. 30, no. 3, pp. 1057–1085, 2014, doi: 10.1193/070113EQS184M.

[26] I. M. Idriss, "An NGA-West2 Empirical Model for Estimating the Horizontal Spectral Values Generated by Shallow Crustal Earthquakes," *Earthq. Spectra*, vol. 30, no. 3, pp. 1–31, 2014, doi: 10.1193/070613EQS195M.

[27] B. S. Chiou and R. R. Youngs, "Update of the Chiou and Youngs NGA Model for the Average Horizontal Component of Peak Ground Motion and Response Spectra," *Earthq. Spectra*, vol. 30, no. 3, pp. 1117–1153, 2014, doi: 10.1193/072813EQS219M.

[28] D. M. Boore, "Orientation-Independent , Nongeometric-Mean Measures of Seismic Intensity from Two Horizontal Components of Motion," *Bull. Seismol. Soc. Am.*, vol. 100, no. 4, pp. 1830–1835, 2010, doi: 10.1785/0120090400.

[29] S. K. Shahi and J. W. Baker, "NGA-West2 Models for Ground-Motion Directionality. Technical Report PEER 2013/10," Berkeley,CA, 2013.

[30] F. McKenna, G. L. Fenves, M. H. Scott, and B. Jeremic, "Open System for Earthquake Engineering Simlation (OpenSees)(Version 3.0.3)." Pacific Earthquake Engineering Research Center, University of California, Berkeley,CA, 2000.

[31] A. K. Chopra and R. K. Goel, "A modal pushover analysis procedure for estimating seismic demands for buildings," *Earthq. Eng. Struct. Dyn.*, vol. 31, no. 3, pp. 561–582, 2002, doi: 10.1002/eqe.144.

[32] C. A. Arteta and J. P. Moehle, "Seismic Performance of a Building Subjected to Intermediate Seismic Shaking," *ACI Structural Journal*, vol. *115,* no. 2.

